ACS FOOD SCIENCE & TECHNOLOGY

pubs.acs.org/acsfoodscitech

Article

Calcium Alginate Beads Loaded with Green Tea Extract: Impact of Drying Methods on Its Structure, Release Behavior, and Storage Stability

Sadaf Parvez and Idrees Ahmed Wani*

Cite This: https://doi.org/10.1021/acsfoodscitech.3c00696

Read Online

ACCESS | Metrics & More | Article Recommendations

ABSTRACT: In this study, calcium alginate beads containing green tea extract were formulated by using oven and freeze-drying methods. Using calcium alginate as a carrier and guar gum as a filler ingredient, the beads were prepared through an ionotropic gelation process. The internal texture of oven-dried beads (ODBs) was more homogeneous and compact than that of the freeze-dried beads (FDBs). Based on texture analysis, the ODBs were harder because their internal structure was more rigid. The FDB showed a greater efficiency of encapsulation (74.98%) than that of the ODB (58.04%). Under alkaline conditions, oven- and freeze-dried beads exhibited higher swelling and release rates than under acidic conditions. It was found that FDB released more polyphenols and had a higher metal chelation activity (85.81%) and radical scavenging power (78.33%) than that of oven-dried beads. Both systems were well-fitted by semiempirical models. In addition, both the ODB and FDB showed a 3-fold increase in bioactivity during storage at room temperature (27 ± 2 °C).

KEYWORDS: *green tea, hydrogels, release kinetics, swelling kinetics, mathematical modelling, storage study*

1. INTRODUCTION

Tea (*Camellia sinensis var. assimica* L) is a popular beverage consumed by millions of people worldwide.[1] Tea has several potential health benefits, including anticancer, antioxidant, and antimicrobial properties. Besides, it decreases the risk of diabetes and coronary artery-related issues. Tea polyphenols are the most abundant bioactive molecules in tea and are responsible for numerous observed bioactivities.[2]

In recent years, a change in the consumption pattern of food has been reported and it has been observed that a vast majority of consumers are inclined to various nutraceuticals and superfoods, particularly green tea polyphenols. These green tea polyphenols can be a base for the formulation of nutraceuticals and superfoods.[3] However, if tea polyphenols are to be used as functional ingredients, then their stability and interaction with food constituents must be considered. Several variables can affect green tea polyphenols (catechins), including the temperature, pH, and oxygen concentration. The bioavailability of tea catechins presents a challenge due to less stability and poor gastrointestinal absorption.[4] Also, a high content of catechins contributes to the bitterness and astringency of green tea. So, the use of encapsulation technologies has been found to improve the stability and controlled delivery of catechins.[5,6]

A variety of approaches have been investigated so far to encapsulate polyphenols, including spray drying,[7,8] coacervation,[9] hydrogels,[10,11] pickering emulsions,[12] liposomes,[13] and nanospheres.[14] One of the most promising approaches for protecting and delivering polyphenols is hydrogel encapsulation. Alginate is the most widely used natural hydrogel to encapsulate bioactive chemicals by ionic gelation.[15,16] Yet, the encapsulated compounds are released rapidly in vitro due to the porous gels formed, which results in low efficiency of encapsulant and fast release.[11] Many studies have used fillers to improve the structures of alginate hydrogels. Fillers have also helped to improve the encapsulation and release capabilities of encapsulated bioactive compounds in a controlled manner. Proteins and polysaccharides[11,17] are the most often utilized fillers. A nonionic polysaccharide (Guar gum) used as a filler material could also be used as a carrier for targeted therapeutic delivery.[18] Once the beads are prepared by gelation, drying is essential for the mechanical strength and storage stability. Many different drying methods are in use today. Drying procedures used in gel manufacture are expected to have a substantial impact on the physical properties of the gel.[19] Moreover, alginate is thermolabile, which necessitates an evaluation of the drying method in bead preparation.

The main contribution of this work is to investigate an efficient method for the encapsulation of green tea extract (GTE) to produce dried beads with a high phenolic content. Furthermore, beads were oven- and freeze-dried to investigate the effect of drying methods on their geometrical, morphological, encapsulation efficiency, swelling, and release kinetics

Received: December 21, 2023
Revised: March 5, 2024
Accepted: March 5, 2024

properties. In addition, the storage study of beads was also examined.

2. MATERIAL AND METHODS

2.1. Materials. *2.1.1. Chemicals.* Sodium alginate (Sigma-Aldrich with molecular weight 80−120 kDa), guar gum, sodium citrate, methanol, acetic acid (product code: RM/065/16; minimum assay: 99.6%), HCl, bile salt (product code: 0194000100; bile acid content: 65%), phosphate buffer, NaOH, Folin−Ciocalteu reagent, ferric chloride, and gallic acid (product code: 83163) were of analytical grade. Pepsin (Hi-Media with product code: 0000300680; activity: ≥ 10000.0 NFU/mg), pancreatin enzyme (Hi-Media with product code: 0000345904; activity: = 3 NF/USP), 2,2-diphenyl-1-picrylhydrazyl (DPPH) (Sigma-Aldrich with product code: 101302233), ferrozine (Hi-Media with product code: 0000357255), 2,4,6-tripyridyl-s-triazine (TPTZ) (Hi-Media with product code: 0000304247) were also procured. Milli Q water (MERCK MILLIPORE) were used throughout the studies.

2.1.2. Collection of Samples. Dried green tea leaves (Mongra II) were collected from the Tea Garden in Assam (Ashapur) in the first and second flushes of the year 2022. The leaves were manually cleaned and stored in containers for further use. All of the chemicals used were of analytical grade. Enzymes and standards were procured from Hi-Media and Sigma-Aldrich, respectively. Double distilled water was used during the entire research.

2.2. Methods. *2.2.1. Tea Extract Preparation.* Extraction of tea polyphenols was carried out under reflux conditions. A reflux condenser was used to extract a specific weight of tea leaves in hot water. When the brewing was complete, the green tea infusion was cooled immediately and filtered through Whatman filter No. 1. The extracts were then centrifuged (Sigma-Aldrich GmbH, Sternheim, Germany) for 10 min at 6000 rpm, again filtered, and then concentrated using a rotary evaporator (Roteva-Equitron, New Delhi, India) at temperatures not exceeding 27 °C. GTE was stored in amber-colored glass bottles at 4 ± 2 °C for subsequent study.

2.2.2. Preparation of Green Tea-Loaded Alginate Blended Hydrogel Beads. The preparation of beads was carried out using the ionotropic gelation approach, following a modified method of Li et al.[20] The primary solution of sodium alginate (5% w/v) and GTE (3% w/v) prepared in distilled water was homogenized using a high-speed homogenizer (Witeg Labortechnik GmbH, Korea) at 10000 rpm for 5 min. A filler solution of guar gum (0.05%) was prepared in aqueous water, added to the primary solution, and stirred in darkness overnight. The mixture was sonicated at 20 kHz frequency and 400 W power by using the fixed probe sonicator (Cole-Parmer, Illinois, USA) for 10 min and left undisturbed for about 2 h for debubbling. From this mixture, 5 mL was dropped into a 5.0% (w/v) calcium chloride aqueous solution using a 21 G needle. The beads formed were washed with distilled water to remove any excess $CaCl_2$ (calcium chloride). The obtained beads were dried by lyophilization (Lyovapor L-200, BUCHI, Germany) at −55 °C, with a vacuum pressure of 0 bar. Some portions of the formed beads were oven-dried (Narang Scientific Works Pvt. Ltd., India) at 25 °C for 24 h and then kept in plastic vials at room temperature for further use. The control beads were prepared without the addition of tea extract and oven-dried.

2.3. Geometric Properties and Moisture Content of Beads. A digital vernier calliper (Aerospace 300 mm Digital Vernier Calliper) with accuracy up to 0.01 mm was used to measure the dimensions of 20 randomly picked beads. The following relationship[21] was used to compute the arithmetic and geometric mean diameter (d_a and d_g) of the beads, where (L) the major, medium (W), and minor (T) are the dimensions of beads. Mean diameter is defined as the average diameter of the beads. As the shape of the beads is not perfectly spherical, three diameters are defined as major, medium, and minor. These diameters are then used to calculate an average diameter defined as d_a and d_g as shown in eq 1) and eq 2).

$$d_a = \frac{(L + W + T)}{3} \tag{1}$$

$$d_g = \sqrt[3]{(LWT)} \tag{2}$$

The sphericity, Φ, of beads was calculated by using eq 3):

$$\Phi = \frac{(LWT)^{1/3}}{L} \tag{3}$$

Surface area and volume of beads was calculated using eq 4) and eq 5), respectively:

$$S = \frac{\pi B L^2}{2L - B} \tag{4}$$

$$V = \frac{\pi B^2 L^2}{6(2L - B)} \tag{5}$$

where $B = (WT)^{0.5}$.

Moisture content of dried beads was measured in triplicate by drying a known amount of beads at 70 °C until constant weight.[22]

2.4. Loose/Aerated and Tapped Bulk Density. Powdered sample (2 g) was gently put into a graduated glass cylinder with a 10 mL capacity to determine the loose/aerated bulk density. The tapped density was determined by manually lifting the cylinder to a height 15 ± 2 mm and dropping it until there was no discernible in the volume of the sample.[23] The sample volume was recorded and measurements were taken in triplicates.

2.5. Colorimetric Analysis. Color measurement of the beads was done by colorimeter (Hunter Lab D25, Hunter associates Lab, Reston, USA), using the CIELAB (L^*, a^*, b^*) system. The instrument was calibrated using a white ceramic plate.

2.6. Encapsulation Efficiency. The encapsulation efficiency was performed according to the previously described study.[5] A known amount of oven and freeze-dried beads were dissolved in a sodium citrate solution (2% w/v) and continuously stirred at ambient temperature, and supernatant was taken for further analysis. The content of polyphenols loaded was assessed using Folin−Ciocalteu's assay (FC), which was slightly modified from a previous work.[24] Blank beads without encapsulated GTE were also assessed for total phenolic content using the FC assay to remove the intervention from coating to calculate the exact GTE content packed in the produced beads. The encapsulation efficiency was calculated by

https://doi.org/10.1021/acsfoodscitech.3c00696
ACS Food Sci. Technol. XXXX, XXX, XXX−XXX

$$\frac{\text{Content of GTE released from beads}}{\text{Total GTE in the initial liquid extract}} \times 100$$

2.7. Morphological Observation of Alginate-Based Beads. *2.7.1. Optical Microscopy.* The morphology of the dry beads was observed in an optical microscope (Lieca 750P, Germany) with the 2.5× and 4× objective lenses.

2.7.2. Scanning Electron Microscopy. A field emission scanning electron microscope (FE-SEM) was used to examine the surface morphology of beads (Gemini SEM 500, ZEISS). Freeze-dried and air-dried beads were fixed to sample stubs to which a conductive tape (double-sided) was attached. The samples were then gold-coated (50 nm) under a vacuum. The coated samples were viewed in FE-SEM with 6 kV accelerating voltage. The samples were analyzed at a 200 μm scale with 100× magnification and at a 100 μm scale with 300× and 200×.

2.8. Fourier Transform Infrared Spectroscopy (FTIR) Analysis. An FTIR spectrometer (FTIR-CARY 630, Agilent Technologies, USA) was used to record the spectra of sodium alginate powder (A), calcium alginate gel beads (CA), lyophilized green tea extract (GTE), GTE air-dried beads (ACGA), and GTE freeze-dried beads (ACGF). To evaluate group frequencies, samples were placed on the ATR glass and scanned in the 4000 to 650 cm^{-1} range.

2.9. X-Ray Diffraction (XRD) Analysis. The crystallographic structure of the beads was investigated by using X-ray diffraction (XRD) patterns. Using a mortar and pestle, a few grams of sample was ground to a fine powder and smeared uniformly over a glass slide with a flat upper surface, producing a random distribution. The operating conditions for observation were X-ray line (λ= 1.542 Å), voltage 4000 V, and 0.03 A current. XRD profiles were recorded in the 2θ range (10−50) using a Shimadzu Lab X-XRD-6100 with a scanning speed of 2.015 deg/min.

2.10. Release Profiles of GTE in the Simulated Gastrointestinal Conditions. GTE-loaded beads were subjected to a model (in vitro digestion) that mimics the digestion process in the model system. The beads (300 mg) were placed in a centrifuge tube containing 15 mL of simulated gastric fluid (SGF). SGF was prepared by mixing 8.571 mol/L pepsin with 0.154 mol/L salt solution and adjusting the pH to 2 with 1.0 mol/L hydrochloric acid. The tubes were kept for incubation at 37 °C in an orbital shaker bath at a 250 rpm speed. Over the period of 3 h, aliquots of 2 mL of supernatant were taken at various intervals. The samples were quickly cooled and stored at −20 °C until further use. After gastric digestion, the mixture was immediately centrifuged (3000 rpm for 5 min), the supernatant liquid was collected, and 15 mL of simulated intestinal fluid (SIF) was added to the residue-undigested matter. SIF was prepared by dissolving 0.007 mol/L bile salts and 0.01 mol/L pancreatic enzyme in buffer solution, and pH was balanced to 7.5 using 0.1 M NaOH solution. The tubes were again kept in an orbital shaker bath at 37 °C and 250 rpm. Over a period of 4 h, aliquots of 2 mL were taken at varying intervals. The separated supernatants were analyzed for different chemical assays to assess the mechanism of GTE release from the encapsulated beads in gastric and intestinal media. To keep the trypsin enzyme inactive, all of the samples were promptly cooled and kept frozen at −20 °C until further use.

2.11. Release Modeling. To assess the mechanism of GTE release from the encapsulated beads in gastric and intestinal media, the data were analyzed by mathematical models presented in section 3.5.

2.12. Antioxidant Assay. *2.12.1. Estimation of Total Phenolic Content (TPC), DPPH Radical Scavenging Activity, Ferric Reducing Power (FRAP), and Metal Chelating Activity (MC).* Antioxidant assays, including Folin−Ciocalteu for total phenolics, DPPH free radical scavenging, and FRAP, were adapted from the methods described by Parvez et al.[25] with specific modifications as detailed below.

Briefly, the assays were conducted spectrometrically (Thermo Scientific, Singapore) using a 96-well plate reader. The Folin−Ciocalteu method was used to quantify the total phenolics. TPC was determined with a calibration curve of gallic acid in the linear range of 20−100 μg/mL (R^2 = 0.99) plotted for the quantification of phenolic compounds and results were expressed as milligrams of gallic acid equivalents per gram of beads (mg GAE/g beads). DPPH inhibition percentage was measured by quantifying the DPPH radical scavenging capacity of different samples. DPPH (0.2 mM) was prepared in methanol, and optical density was determined at 517 nm. Antioxidant assay by FRAP was measured by preparing FRAP reagent, in the proportion 1:1:10 (v/v/v); 10 mM TPTZ was added to 0.04 M hydrochloric acid, 0.02 M $FeCl_3$, and 0.3 M acetate buffer (pH 3.6) and absorbance was measured at λ = 593 nm. Metal chelating activity was determined at λ= 562 nm with EDTA as the positive control.

2.13. Swelling Studies. To study the swelling properties of dry beads, they were first immersed in distilled water. Then the beads were put in falcon tubes in the dry state containing 10 mL of release medium, which was incubated at 37 °C with shaking at 200 rpm. At first, dry beads were swollen in SGF at pH 2 for 4 h. Afterward, the beads were shifted to SIF at pH 7.5 for the next 4 h. Beads were removed from the swelling solution at predetermined intervals, and excess water from the surface was absorbed with the filter paper. The sample weight (W_t) at a certain time t and dry weight of the sample (W_d) were used to calculate the degree of swelling $S(t)$. Each analysis was carried out three times.[26]

$$S(t) = \frac{W_t - W_d}{W_d}$$

2.14. Storage Stability of Alginate-based Beads. Beads were kept in falcon tubes covered by aluminum foil and stored in the dark environment at an ambient temperature (27 ± 2 °C), and the same were studied for over 6 months. The beads were analyzed for TPC, FRAP, ABTS, and DPPH assays under simulated in vitro gastrointestinal conditions.

2.15. Texture Analysis. The texture analysis of the beads was performed by a texture analyzer (TA.XT Plus texture analyzer, Stable Micro systems). In the compression test, a 75 mm probe of cylindrical shape and a load cell weighing 5 kg were used. The samples were analyzed at a distance of 2 mm and a speed of 0.5 mm/s (half of sample thickness). The tests were conducted at room temperature (27 ± 2 °C). The greatest force (N) required for compression is the indication of the sample's hardness. This force measures the maximum resistance of surface to probe compression. The total distance traversed by the probe up to the breaking point of each sample was used to determine the elasticity. Every analysis was carried out in triplicate (on different beads). Texture Exponent 5.0 Software (Stable Micro Systems, Great Britain) was used to calculate all of the maximum peak calculations.

https://doi.org/10.1021/acsfoodscitech.3c00696
ACS Food Sci. Technol. XXXX, XXX, XXX−XXX

Table 1. Geometric Properties of Oven-Dried (OD), Freeze-Dried (FD), and Control Hydrogel Beads (C)[I]

sample	L (mm)	W (mm)	T (mm)	d_a (mm)	d_g (mm)	Φ (%)	S (mm^2)	V (mm^3)	MC (%)	Hardness (N)	Cohesiveness
OD	1.75 ± 0.17^a	1.32 ± 0.03^a	1.03 ± 0.06^a	1.37 ± 0.07^a	1.34 ± 0.7^a	76.66 ± 4.43^a	4.84 ± 0.44^a	0.94 ± 0.12^a	11.15 ± 0.30^b	126.22 ± 11.90^b	0.87 ± 0.09^b
FD	5.27 ± 0.25^b	4.7 ± 0.44^c	4.27 ± 0.60^b	4.74 ± 0.43^c	4.72 ± 0.43^c	89.57 ± 3.97^b	64.96 ± 13.5^b	49.21 ± 15.29^b	17.41 ± 0.37^c	9.65 ± 0.24^a	0.08 ± 0.01^a
C	1.97 ± 0.12^a	1.83 ± 0.06^b	1.63 ± 0.23^a	1.81 ± 0.14^b	1.80 ± 0.14^b	91.70 ± 1.6^b	9.58 ± 1.62^a	2.79 ± 0.73^a	12.58 ± 0.07^a	134.14 ± 0.23^b	0.84 ± 0.02^b
wet beads	5.71 ± 0.01^c	5.60 ± 0.02^d	5.52 ± 0.03^c	16.83 ± 0.05^d	5.61 ± 0.02^d	98.24 ± 0.16^c	97.18 ± 0.75^c	90.05 ± 1.05^c			

[I]Different letters (a, b, c, d) in the same column indicate significant differences between mean values ($p \leq 0.05$). Values are means with standard deviation; OD: oven-dried, FD: freeze-dried, C: control; L = major; W = medium; T = minor; d_a= arithmetic mean diameter; d_g= geometric mean diameter; Φ= sphericity; S = surface area; V = volume, MC = moisture content.

2.16. Statistical Analysis. The analysis was repeated three times for each sample to calculate the average and standard deviation. One-way ANOVA was used to analyze the data with the Duncan test and Student's t tes at a 95% confidence interval.

3. RESULTS AND DISCUSSION

3.1. Geometric Properties. Geometric properties of the beads are listed in Table 1. On examining the various bead parameters like geometric diameter (d_g), arithmetic mean diameter (d_a), volume, and surface area, it was observed that the numerical values of these parameters were greater in freeze-dried beads than in oven-dried and control beads. However, sphericity was seen more in control than the beads with encapsulate. A similar trend was also seen for moisture content with 17.41% ± 0.37 for freeze-dried beads and 12.58% ± 0.07 for air-dried beads (Table 1). Wet beads had an average diameter of 16.85 ± 0.05 mm. Drying of the beads resulted in their shrinkage. There was more shrinkage in oven-dried alginate beads (1.37 ± 0.17 mm d_a) than in the freeze-dried beads (4.74 ± 0.43 mm d_a). In general, significant ($p \leq 0.05$) differences were noted in the geometric properties of beads. The beads prepared min^{-1} was 34 ± 4.36. The reasons for these differences involve the distinct drying mechanisms and their impact on the alginate network. As a result of the slower sublimation process of freeze-drying, there are fewer internal stresses and ice crystals are formed, resulting in smaller shrinkage. In contrast, rapid water evaporation in an oven may result in internal stresses, which may cause the polymer network to collapse. This likely contributes to a more pronounced shrinkage in oven-dried beads when compared to vacuum-dried beads as reported by Abubakr et al.[32]

Results of texture profile analysis revealed that the hardness was the highest in control beads (134.34 N) followed by oven-dried and freeze-dried beads (Table 1). Cohesiveness of the beads was observed in the range of 0.08−0.87. Significant ($p > 0.05$) differences were observed in hardness and cohesiveness between the oven-dried and freeze-dried beads. However, the difference was not significant ($p > 0.05$) between oven-dried and control beads. The marked difference between the hardness and cohesiveness of beads can be attributed to their internal structure. The freeze-dried beads have a porous structure compared to the beads prepared by oven drying, which have a denser and compact structure.

The CIELAB color coordinates of the oven- and freeze-dried beads are given in Table 2. Comparing the L^* values, which signify lightness, it is evident that freeze-dried beads exhibited a greater degree of lightness compared to oven-dried beads.

Table 2. Encapsulation Efficiency and Color Parameters of Dried Beads[I]

sample	EE (%)	L^*	a^*	b^*	chroma	hue
OD	58.04 ± 3.522^a	7.67 ± 0.12^a	2.97 ± 0.04^a	40.75 ± 0.1^a	40.86 ± 0.11^a	85.83 ± 0.00^a
FD	75.98 ± 0.003^a	12.69 ± 0.16^a	3.40 ± 0.43^a	49.41 ± 0.1^a	49.53 ± 0.07^a	86.06 ± 0.01^b

[I]Different letters (a, b) in the same column indicate significant differences between mean values ($p \leq 0.05$) Values are means with standard deviation. OD: oven-dried, FD: freeze-dried.

This suggests that freeze-drying preserved the original color of the beads to a slightly greater extent. Additionally, the L^* values indicated reduced susceptibility to browning in freeze-dried samples due to subzero temperature employed.

Furthermore, positive values for a^* and b^* denote the contribution for red and yellow color, respectively. Slightly higher values for a^* and b^* along with the highest hue value were obtained for freeze-dried beads, potentially due to the absence of the Maillard reactions (browning) that can occur at higher temperatures in oven drying.

3.2. Encapsulation Efficiency. The high encapsulation efficiency (EE) of dried hydrogel beads could be attributed to the alginate/guar gum gels. The gels show reduced porosity, and their protein may react with tea polyphenols (TP), preventing TP from leach during the making of beads. It was also found that when alginate is coupled with natural polysaccharides and protein, the encapsulation of bioactive compounds can be enhanced efficiently.[5,17,20] EE in oven- and freeze-dried beads was 58.04 ± 3.52 and 75.98 ± 0.003%, respectively (Table 2). The increase in encapsulation efficiency in freeze-dried beads can be attributed to low temperature during the drying process[27,28] and also to the larger bead size than the oven-dried beads.

3.3. Beads Characterization. Photographs of dried hydrogel beads taken by optical microscopy in Figure 1 show that control beads in Figure 1C had a regular, spherical shape. However, beads loaded with GTE had an irregular shape. Oven-dried beads in Figure 1B had slightly irregular shapes, while the freeze-dried beads had several edges with more irregularity in Figure 1A.

Lyophilization would have resulted in the production of flat structures due to the loss of water, which causes the walls of the pores to collapse, which makes the beads slightly flattened.[29,30,31] The control beads were more translucent, whereas the beads that were filled with GTE appeared to be darker. The dark color of the encapsulated beads may be due to the dark color of the encapsulate as reported by Parvez et

https://doi.org/10.1021/acsfoodscitech.3c00696
ACS Food Sci. Technol. XXXX, XXX, XXX−XXX

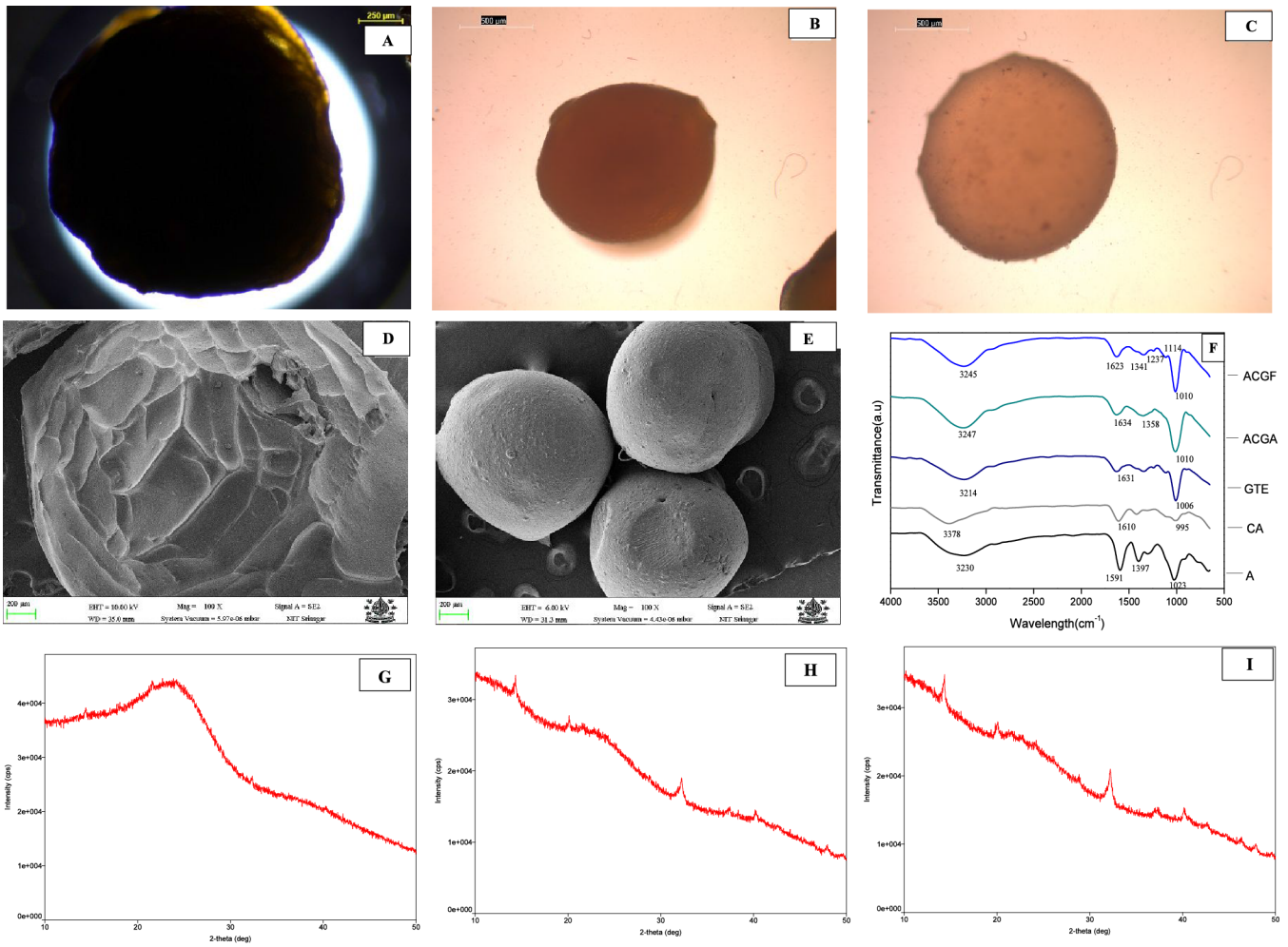

Figure 1. Structural characterization; optical microscopy images of (A) freeze-dried, (B) oven-dried and (C) control beads. Scanning electron micrographs of (D) freeze-dried, (E) oven-dried; (F) FTIR spectra of sodium alginate powder (A), calcium alginate gel beads (CA), lyophilized green tea extract (GTE), and GTE air-dried beads (ACGA) and GTE freeze-dried beads (ACGF) XRD patterns of (G) freeze-dried, (H) oven-dried, and (I) green tea extract.

al.[25] The freeze-dried beads were larger compared with the oven-dried and control beads. This is because of the greater porosity of freeze-dried beads as revealed by scanning electron micrographs.

The shape and surface characteristics of the beads were studied using SEM. These characteristics are critical for the release of encapsulates. The SEM images of freeze-dried beads show a honeycomb-like structure with porous interiors. These are created by the sublimation of ice from minute ice crystals leading to the formation of voids (Figure 1D). The air-dried beads, however, showed a smooth surface with no pores (Figure 1E). SEM images revealed that oven-dried beads showed desirable shape and size. The results showed that air drying resulted in more spherical beads with a smooth surface.

The FTIR technique was utilized for the characterization and identification of functional groups and matrix−GTE compound interaction. The noncovalent interactions of sodium alginate powder (A), calcium alginate gel beads (CA), lyophilized green tea extract (GTE), GTE air-dried beads (ACGA), and GTE freeze-dried beads (ACGF) were found based on the spectra of FTIR spectrometer. As illustrated in Figure 1F, the spectrum of A powder reveals peaks at about 1023, 1591, 1397, and 3230 cm^{-1}, corresponding to C−O−C, COO^- (asymmetric), COO^- (symmetric), and O−H stretching, respectively. These observations were consistent with prior findings.[15] A major absorption band is observed at 3378.93 cm^{-1} originating from the O−H stretching. The shift of the OH stretching peak to a higher wavenumber is due to the cross-linking process of CA.

FTIR spectra of encapsulated GTE differed from the spectra of control beads, indicating encapsulation of GTE. The FTIR spectra for the CA and encapsulated beads prepared by the oven- and freeze-drying showed minimal variation in the range of 1000−1600 cm^{-1}. After the production of air- and freeze-dried GTE beads, the peak of hydroxyl bond (O−H) in GTE (3230 cm^{-1}) and alginate (3214 cm^{-1}) changed slightly to higher values (3247 and 3245 cm^{-1} respectively). When GTE was encapsulated into the alginate beads, a significant shift to lower wavenumber was observed for the O−H functional group implying that hydrogen bonding created intermolecular interaction between alginate and GTE. Furthermore, the intensity of peaks 1237 cm^{-1} (C−O vibration of alcohols, ethers, carboxylic acids, and esters) and 1623 and 1634 cm^{-1} (C−C carbon−carbon aromatic double bond stretching) increased in the alginate bead spectra after incorporation with GTE compounds. This formation of hydrogel alginate beads with GTE did not affect the new peaks. Therefore, it could be envisaged that no chemical interaction occurred

https://doi.org/10.1021/acsfoodscitech.3c00696
ACS Food Sci. Technol. XXXX, XXX, XXX−XXX

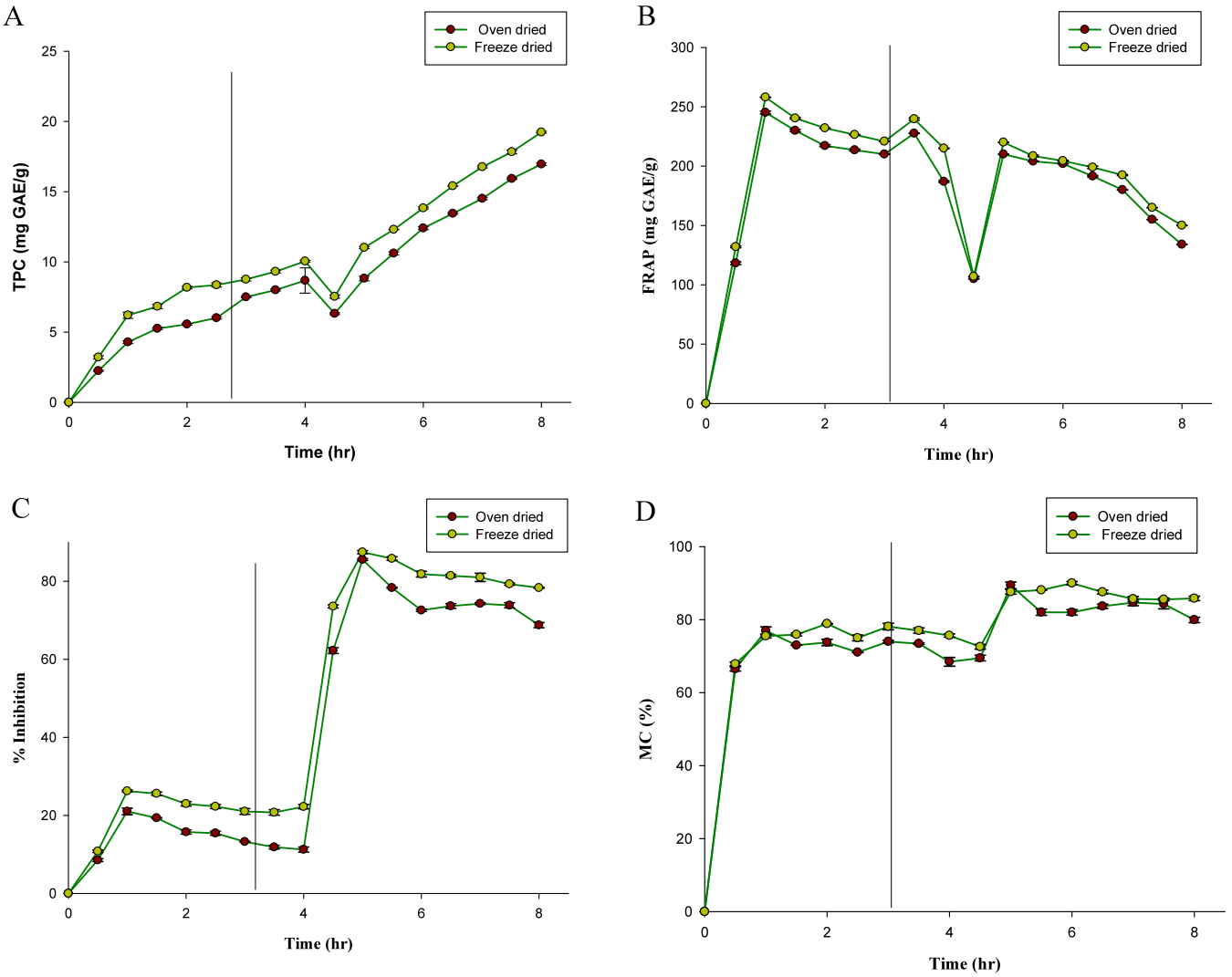

Figure 2. In vitro gastro intestinal release and swelling kinetics of hydrogel beads; (A) release profiles of total phenolic content (TPC) of oven-dried and freeze-dried beads under simulated gastro intestinal conditions; (B) ferric reducing activity (FRAP) of oven-dried and freeze-dried beads under simulated gastro intestinal conditions. (C) Radical scavenging activity (DPPH) of oven-dried and freeze-dried beads under simulated gastrointestinal conditions. (D) Metal chelating activity (MC) of oven-dried and freeze-dried beads in gastrointestinal conditions.

between the GTE and alginate beads. There might be overlapping of GTE peaks and the alginate (used as wall material) peaks of the FTIR spectra. The lack of chemical interaction between the phytochemicals of GTE and alginate was consistent with previous studies.[29] Consequently, whether freeze-dried or oven-dried, the calcium alginate bead provides a biocompatible material for encapsulating bioactive components of GTE.

XRD patterns of dried GTE, oven-, and freeze-dried beads are presented in Figure 1. Oven- (Figure 1G) and freeze-dried beads (Figure 1H) showed peaks almost at similar diffraction angles of 2θ with intensities of 14.35, 20.12, 22.89, 32.19, 37.23, 40.20, 46.28, and 47.89, indicating the crystalline nature of the beads. The XRD pattern of GTE in Figure 1I revealed a significant broad peak (2θ), suggesting that GTE predominantly exists in an amorphous state. Thus, from the XRD pattern of the GTE-loaded beads, it can be inferred that the GTE was not present in an amorphous state in the bead matrix but was in the crystalline state. This indicates that the change in the amorphous state of the GTE[43] occurred during the bead preparation by this ionotropic gelation method.

3.4. Release Kinetics of Green Tea Polyphenols in Simulated Digestive Fluids. To evaluate the neutraceutical potential of the beads, in vitro release tests were conducted at pH 2 for 4 h and then at pH 7.5 for 4 h to simulate gastric and intestinal fluids, respectively. All of these release studies were carried out at 37 °C which is the normal temperature of the human body. Calcium alginate gels were reinforced with guar gum as a filler material in this study to inhibit the quick release from alginate gels. The incorporation of filler materials aided in the sustained release under both SGF and SIF conditions. In our study, nearly a gradual release was observed throughout 240 min in SGF, followed by a constant release in SIF. Overall, the freeze-dried beads released significantly more GTE than the oven-dried beads at pH 2 and 7.5, respectively. Since it has been stated that large particle-sized beads prolong the delivery of the active compounds, the release profile of the active compound from the delivery system is also prolonged.[29] In our case also, the freeze-dried beads exhibited a prolonged and greater release profile than oven-dried beads as the latter had larger particle size.

https://doi.org/10.1021/acsfoodscitech.3c00696
ACS Food Sci. Technol. XXXX, XXX, XXX−XXX

Table 3. Kinetic Parameters Obtained from the Semi-Empirical Models

	first order		Korsmeyer−Peppas model			Higuchi model		Peppas Shalin			
condition	K_1	R^2	K_{kp}	R^2	n	K_H	R^2	K_1	K2	R^2	transport mechanism
ODG	0.02	0.86	3.88	0.99	0.57	4.17	0.98	3.93	−0.05	0.98	anomalous transport
FDG	0.03	0.69	5.59	0.98	0.43	5.23	0.97	6.72	−1.15	0.98	Fickian
ODI	0.05	0.79	8.77	0.99	0.47	8.54	0.99	8.7	0.08	0.99	anomalous transport
FDI	0.06	0.74	10.41	0.99	0.43	9.78	0.99	9.7	0.72	0.99	Fickian

Different release rates were achieved from the oven and freeze-dried beads. According to our findings, freeze-dried beads showed a quick release in both simulated intestinal and gastric fluids, while oven-dried beads had release kinetics slower than those of freeze-dried beads. The quick release of the freeze-dried beads can be attributed to the more porous structure (due to ice sublimation) that occurs after freeze-drying. As a result of higher solvent uptake,[32] freeze-dried beads degrade more swiftly in the dissolving medium, and the same is concluded by swelling kinetics.

GTE release kinetics of the beads is presented in Figure 2. As shown, for TPC Figure 2A the maximum release of GTE at a pH value of 2 for oven-dried beads was 8.67 mg of GAE/g and 10.04 mg of GAE/g for freeze-dried beads. The limited swelling degree from the oven- and freeze-dried beads results in a delayed release at pH 2. The release of GTE at pH 7.5 increased significantly in correspondence with an increased degree of swelling of the alginate gel network (16.95 and 19.2 mg GAE/g for oven- and freeze-dried beads, respectively).

Reducing power ability of GTE at pH 2 for oven-dried beads was 187 mg GAE/g and 215 mgGAE/g for freeze-dried beads (Figure 2B). However, at pH 7.5 reducing power capacity reduced significantly for both oven- and freeze-dried beads (134 and 150 mg GAE/g, respectively). The antioxidant property of phenolics is pH-dependent. Under alkaline conditions, Fe^{3+} ions would have reacted more with available OH ions as compared to polyphenols, thus resulting in a decrease in reducing power ability. The modifications in pH can lead to alterations in structure and confirmation of phenolic compounds, consequently affecting antioxidant activity. Findings presented in this paper are in agreement with studies by Arenas and Trinidad[33] and Flores and Kong[34] who reported a similar trend using the FRAP method to evaluate antioxidant activity in fresh apples at different points of simulated digestion.

Metal chelating activity of oven-dried and freeze-dried beads under simulated gastric conditions (pH 2) was 68.44% and 75.66%, respectively (Figure 2C). In simulated intestinal conditions, the metal chelating activity of 79.6% and 85.81% was shown by oven-dried and freeze-dried beads, respectively.

The DPPH (2,2-diphenyl-1-picrylhydrazyl) assay is a widely used method to assess the radical scavenging activity of antioxidants. It relies on the characteristic purple color of the DPPH radical, which gets reduced when antioxidants donate a hydrogen atom, converting the radical to a stable form. The decrease in the absorbance at 517 nm is directly proportional to the antioxidant activity of the sample.

Green tea extract (GTE) is rich in polyphenols, particularly flavonoids and catechins, which possess hydroxyl groups that readily donate hydrogen atoms to the DPPH radical, neutralizing it and contributing to the observed decrease in absorbance.

The drying method used can potentially influence the interaction of GTE with DPPH and its observed antioxidant activity. The higher temperatures during oven drying may partially degrade some heat-sensitive antioxidant compounds in GTE. This could reduce the number of available hydrogen atom donors and consequently lower the observed DPPH scavenging activity. The subzero conditions of freeze-drying might preserve the native structure of GTE molecules, allowing for better accessibility of the DPPH radical to the hydrogen atoms present. This could potentially lead to higher observed DPPH scavenging activity compared with oven-dried samples. In our analysis, DPPH activity (Figure 2D) of the beads showed sustained radical scavenging activity in both gastric and intestinal conditions. The scavenging activity increased significantly at pH 7.5 (68.77% and 78.33%). The presence of alginate promotes the formation of a gelatinous layer following the hydration, which can act as a polyphenol diffusion barrier and may constrict to sustained release in simulated intestinal conditions. Similar results were reported by Arenas and Trinidad[33] for DPPH and ABTS activity

3.5. Mathematical Modeling of Gelled Beads. To understand the mechanism of release GTE from beads, the experimental data were analyzed by first order eq (eq 6), Korsmeyer−Peppas (eq 7), Higuchi (eq 8), and Peppas−Sahlin model (eq 9):

$$M_t = M_O e^{-k1t} \tag{6}$$

where (M_t/M_o) is the ratio of released mass at time t (M_t) to the maximum mass of polyphenols (M_o) released at time $t = \infty$ in all conditions and the first-order rate k_1 constant.

$$\frac{M_t}{M_\infty} = kt^n \tag{7}$$

$\frac{M_t}{M_\infty}$: the fraction released at time t, the rate constant k (which depends on structural changes and geometry of the system).

The release exponent (n) is dependent on release mechanism

$$f_1 = M_t = K_H\sqrt{t} \tag{8}$$

The dissolving constant (concentration per time 1/2) is denoted by K_H

$$\frac{M_t}{M_\infty} = k_1 t^{0.5} + k_2 t \tag{9}$$

where k_1 and k_2 are equation constants with k_1 denoting Fickian diffusion, and k_2 is the polymeric chain relaxation/dissolution. The comparison of k_1 and k_2 may reveal information regarding which mechanism is dominant: if $k_1 > k_2$, the active compound release is primarily dictated by diffusion, else erosion is the key associated phenomenon, considering the possibility of two separate mechanisms functioning simultaneously.

https://doi.org/10.1021/acsfoodscitech.3c00696
ACS Food Sci. Technol. XXXX, XXX, XXX−XXX

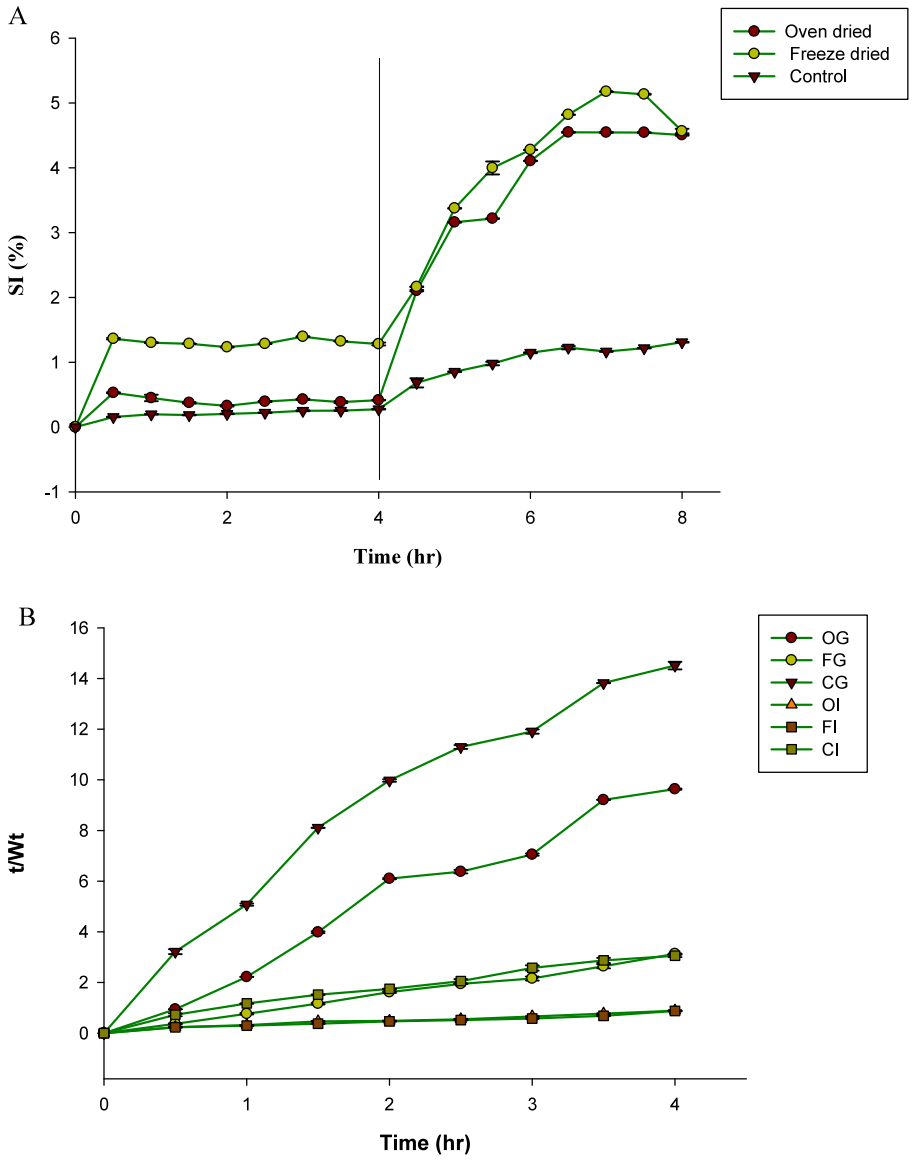

Figure 3. (A) Swelling behavior in simulated gastric and intestinal fluid for oven-dried, freeze-dried, and control beads; (B) effect of time on the swelling ratio of oven-dried gastric (OG), freeze-dried gastric (FG), control gastric (CG), oven-dried intestinal (OI), freeze-dried intestinal (FI), control intestinal (CI).

Table 3 lists the regression parameters, such as the coefficient of determination (R^2) and release kinetic constants (k). It was shown that Koresmeyer–Peppas, Peppas–Sahlin, and Higuchi showed a good correlation with the release behavior of beads. Almost 90% of the release was determined using the calculation of k and n. A Fickian diffusion release is inferred for spheres, if $n \sim 0.43$; for the range $0.43 < n < 0.85$, it is a non-Fickian diffusion release also known as anomalous transport where drug release is followed both by diffusion and swelling controlled mechanisms. When $n > 0.85$, it specifies polymer relaxation and disentanglement of chains that is related to polymer relaxation of chains or swelling controlled release of a non-Fickian (case II transport).[35] In this study, the values of n are in the range of 0.43–0.85. Oven-dried beads had n values of 0.57 and 0.47, while freeze-dried beads had n values of 0.43 and 0.43 under gastric and intestinal conditions, respectively. This indicates that drug release is a function of both diffusion and swelling in the case of oven-dried beads. Fickian/diffusion type release was indicated by the values of 0.43 for freeze-dried beads. The use of Peppas and Sahlin's empirical equation to analyze the release data further proved that diffusion dominated for freeze-dried beads. Although the relaxation mechanism was also considered, the correlation between the two constants ($k_1 > k_2$) indicates that diffusion is the main release mechanism.

3.6. Swelling Studies. The immersion of beads (control, oven-dried, and freeze-dried) in deionized water for 8 h did not swell the beads. The formation of egg boxes that bind across alginate beads is thought to be the cause of gelation in the presence of calcium (Ca) ions. In the aqueous medium of the gel network, calcium ions are abundant as free ions, in addition to being implicated in egg-box junction zones. In presence of Ca^{2+}, the alginate network shows structural collapse and shrinkage when dried, allowing egg-box junction to come close enough and form lateral aggregations. This causes the dried alginate gel structure to become highly dense by increasing the cross-linking density. This is why the swelling of gel beads hardly occurs in pure water.

https://doi.org/10.1021/acsfoodscitech.3c00696
ACS Food Sci. Technol. XXXX, XXX, XXX–XXX

The development of a strong hydrophilic hydrogen bond between carboxylic and −OH groups of alginate and polyphenolic polar groups at pH 2 reduced the degree of swelling of the beads. Because of the defined enzymatic degradation at pH 2, the beads would remain intact. The beads swelled to their greatest extent in 30 min at this pH and then shrank gradually to their equilibrium state. The beads swelled as the hydrophilic groups were hydrated, a process that differs from the side-by-side aggregations mediated by free Ca^{2+}. When the alginate network is dried, the egg-box junctions grow sufficiently close to form lateral aggregations and the alginate network shrinks and collapses. To explain this phenomenon, we can attribute it to the protonation of carboxylic groups, reducing the chemical potential of the network.

The higher water penetration and degree of swelling seen at pH 7.5 were likely due to the relaxation of polymer chains, which increased the electrostatic force of repulsion between the carboxylic groups.[35] Due to the breakdown and dissolution of the hydrogel network, the maximum degree of swelling was attained, which then declined. Furthermore, divalent Ca^{2+} ions available in alginate beads rapidly exchange with Na^{+} ions in phosphate buffer, resulting in disintegration, as described by Tavakol et al.[36] and Scholt[37] who noted the complete disintegration of alginate beads in phosphate buffer at pH 7 after 2 h.

The influence of pH value on the overall swelling behavior of beads is shown in Figure 3A. Because of their sponge-like structure, the degree of swelling of freeze-dried beads was stronger compared to oven-dried beads at two different pH levels. Such results were also confirmed by Rayment et al.[26] and Tavakol et al.[36] At pH 2, the maximum swelling degree was 0.28, 0.53, and 1.36 for control, oven, and freeze-dried beads, respectively. The corresponding values at pH 7.5 were 1.31, 4.55, and 5.17, respectively.

Bead swelling profiles fitted to a proposed second-order Scholt equation[38,39] (eq 1 and Table 4)

$$\frac{dS_t}{dT} = k_2(S_\infty - S_t)^2 \tag{10}$$

where the proportion of medium absorbed at time a certain t is denoted by S_t, the swelling rate constant is denoted by k_2 and the maximum percentage of medium absorbed at equilibrium is denoted by S_∞. eq 10 was transformed to eq 11 by integrating the aforementioned equation between the limits $t = 0$, $S_t = 0$ and $t = \infty$, $S = S_\infty$,

Table 4. Parameters Obtained From Schott's Equation

sample	A	B	$k_2 \times 10^2/(hr^{-1})$	$1/B$ (SI)	R^2
ODG	0.05	2.50	1.18	0.39	0.98
FDG	0.01	0.77	0.51	1.31	0.99
CG	2.47	3.22	0.04	0.30	0.97
ODI	0.14	0.17	0.002	5.63	0.98
FDI	0.12	0.16	0.002	5.91	0.98
CI	0.44	0.68	0.01	1.48	0.98
sample	A	B	swell ratio = $1/B$		R^2
ODG	0.053	2.506	0.40		0.990
FDG	0.011	0.761	1.31		0.998
CG	2.474	3.229	0.31		0.979
ODI	0.147	0.178	5.62		0.984
ODI	0.123	0.169	5.91		0.981
CI	0.449	0.674	1.48		0.990

$$\frac{t}{S_t} = A + Bt \tag{11}$$

where $A = 1/k_2$, where k_2 is the initial swelling rate of the bead; $B = 1/S_\infty$, where S_∞ is the predicted equilibrium swelling ratio of the bead. As a result, k_2, the Schott kinetic rate constant of swelling, may be obtained as follows:

$$k_2 = \frac{B_2}{A}$$

The following equation was used to determine the swelling ratio at time t

$$S_t\ (g/g) = \frac{W_{t-W_d}}{W_d} \tag{12}$$

where W_t (g) is the weight of swollen beads at time t (min) and W_d (g) is the weight of dry beads.

Figure 3B shows graph t/W_t vs t, for air-dried and freeze-dried beads. The curves obtained had a good fit, and acceptable linear correlation ($R^2 > 0.98$), revealing that the process of swelling fits the Schott's second-order dynamic equation (Table 4). López-Córdoba et al.[10] found similar results when they calculated $R^2 > 0.98$ for their kinetic parameters.

3.7. Storage Stability of GTE−Alginate Beads. There are no earlier studies, to the author's knowledge, on the storage study of green tea polyphenolic extracts encapsulated by ionic gelation. The storage stability of encapsulated GTE in beads prepared by two different drying methods was studied at ambient temperature for 6 months. Figure 4A−D shows the analysis of TPC and antioxidant activity using different assays under in vitro gastrointestinal conditions. Both drying methods preserved the antioxidant capacity and TPC throughout the storage, implying that sodium alginate in combination with the filler material guar gum may have a beneficial impact on the bioavailability of encapsulated phenolic compounds present in tea extract. An increase in the number of polyphenols during storage may be due to the hydrolysis of polyphenol conjugates. The current findings are consistent with prior research,[40,41] which revealed that sodium alginate is a better encapsulating matrix for cactus pear and resulted in higher recoveries and the production of polyphenols. Overall, the freeze-dried beads showed the highest activity under simulated intestinal conditions for all assays when compared with oven-dried beads. The burst effect could explain the rapid release of polyphenols after 6 months of storage. Belščak-Cvitanović et al.[17] suggested that the burst release of polyphenols was due to the release of polyphenols loosely adhered on the matrix surface or due to adsorption on the surface and releasing rapidly from the alginate network due to the inherent porosity. Furthermore, polyphenols on the upper surface layer of the polymeric matrix may escape through these pores, augmenting the initial release. The burst effect was stronger in the case of freeze-dried beads, which could be ascribed to its drying process: during dehydration water moves to the surface, allowing hydrophilic compounds to diffuse and migrate more easily, resulting in an irregular distribution of phenols with larger concentrations on the upper surface of beads.[5] However, antioxidant stability as evaluated by the FRAP technique showed the highest release in simulated gastric conditions for freeze-dried beads. Belščak-Cvitanović et al.[42] reported that the stability of antioxidants in encapsulated plant extract evaluated

https://doi.org/10.1021/acsfoodscitech.3c00696
ACS Food Sci. Technol. XXXX, XXX, XXX−XXX

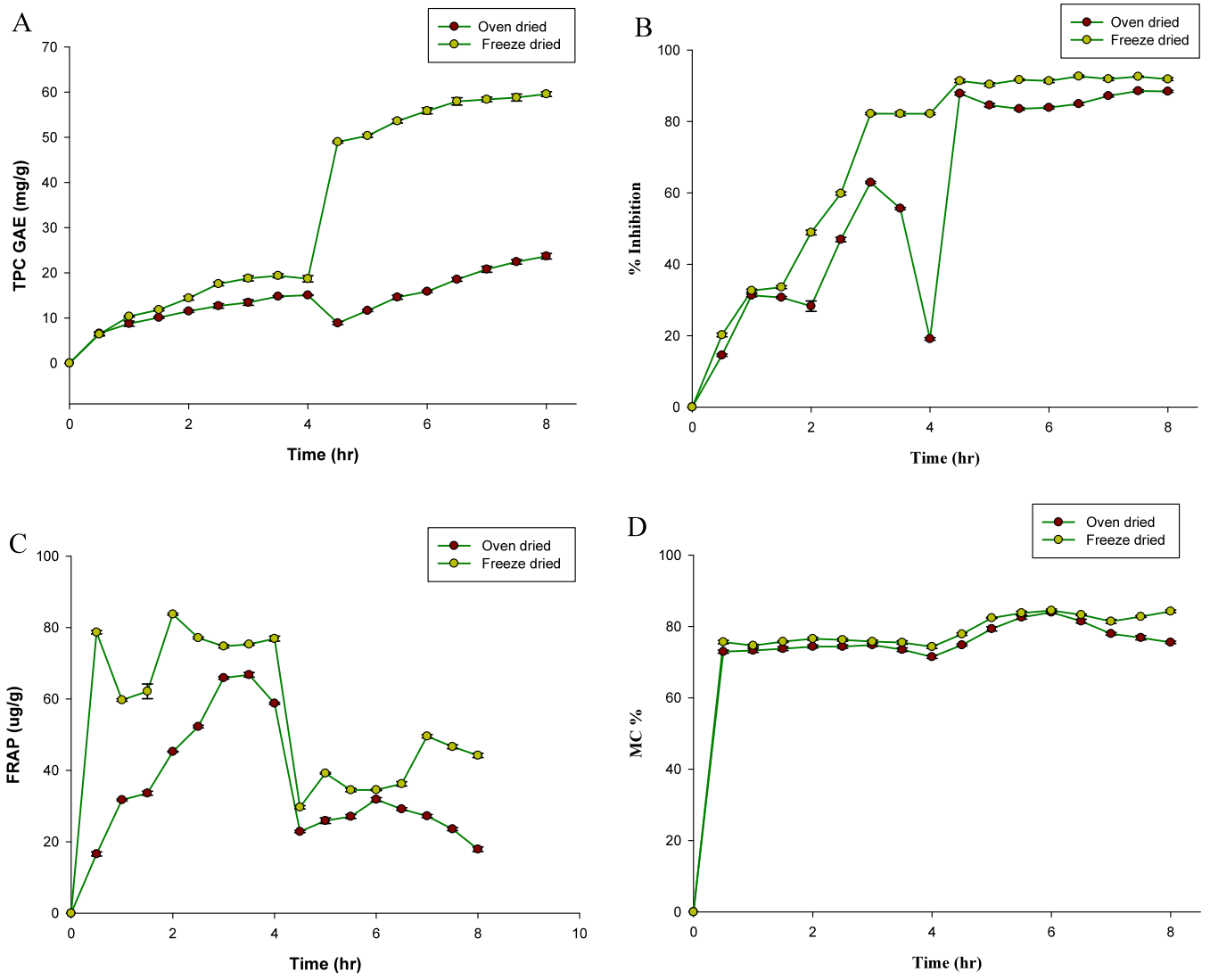

Figure 4. Storage study; (A) release kinetics of oven-dried and freeze-dried beads for total polyphenols (TPC) in simulated gastrointestinal conditions; (B) release kinetics of oven-dried and freeze-dried beads for ferric reducing activity (FRAP) in simulated gastrointestinal conditions; (C) release kinetics of oven-dried and freeze-dried beads for radical scavenging activity (DPPH) in simulated gastrointestinal conditions; (D) release kinetics of oven-dried and freeze-dried beads for metal chelating activity in gastrointestinal conditions.

by the ABTS assay decreased considerably after storage for 2 weeks at 4 °C.

■ ASSOCIATED CONTENT

Data Availability Statement

Data will be available on request.

■ AUTHOR INFORMATION

Corresponding Author

Idrees Ahmed Wani − *Department of Food Science & Technology, University of Kashmir, Srinagar 190006, India*; Phone: +91 7006684149; Email: idwani07@gmail.com; Fax: +91-194-2425195

Author

Sadaf Parvez − *Department of Food Science & Technology, University of Kashmir, Srinagar 190006, India*; orcid.org/0000-0002-2898-5687

Complete contact information is available at: https://pubs.acs.org/10.1021/acsfoodscitech.3c00696

Author Contributions

S.P.: Conceptualization, Data curation, Formal analysis, Validation, Methodology, Software, Writing−original draft. I.A.W.: Conceptualization, Formal analysis, Investigation, Project administration, Resources, Supervision, Visualization, Writing−review and editing. All authors reviewed the manuscript.

Funding

No funding was received.

Notes

The authors declare no competing financial interest.

■ ACKNOWLEDGMENTS

The Council of Scientific and Industrial Research board (CSIR), New Delhi, India is thankfully acknowledged for senior research fellow (SRF) Grant (09/251(0099)2K18 EMR-I) in favor of S.P.

REFERENCES

(1) Zhou, Y.; Yao, Q.; Zhang, T.; Chen, X.; Wu, Z.; Zhang, N.; Shao, Y.; Cheng, Y. Antibacterial Activity and Mechanism of Green Tea Polysaccharide Conjugates against *Escherichia Coli*. *Ind. Crops Prod.* **2020**, *152*, 112464.

(2) Nie, S. P.; Xie, M. Y. A Review on the Isolation and Structure of Tea Polysaccharides and Their Bioactivities. *Food Hydrocolloids* **2011**, *25* (2), 144−149.

(3) Lorenzo, J. M.; Munekata, P. E. S. Phenolic Compounds of Green Tea: Health Benefits and Technological Application in Food. *Asian Pac. J. Trop. Biomed.* **2016**, *6* (8), 709−719.

(4) de Vos, P.; Faas, M. M.; Spasojevic, M.; Sikkema, J. Encapsulation for Preservation of Functionality and Targeted Delivery of Bioactive Food Components. *Int. Dairy J.* **2010**, *20* (4), 292−302.

(5) Belščak-Cvitanović, A.; Dordević, V.; Karlović, S.; Pavlović, V.; Komes, D.; Ježek, D.; Bugarski, B.; Nedović, V. Protein-Reinforced and Chitosan-Pectin Coated Alginate Microparticles for Delivery of Flavan-3-Ol Antioxidants and Caffeine from Green Tea Extract. *Food Hydrocolloids* **2015**, *51*, 361−374.

(6) Borgogna, M.; Bellich, B.; Zorzin, L.; Lapasin, R.; Cesàro, A. Food Microencapsulation of Bioactive Compounds: Rheological and Thermal Characterisation of Non-Conventional Gelling System. *Food Chem.* **2010**, *122* (2), 416−423.

(7) Rezende, Y. R. R. S.; Nogueira, J. P.; Narain, N. Microencapsulation of Extracts of Bioactive Compounds Obtained from Acerola (Malpighia Emarginata DC) Pulp and Residue by Spray and Freeze Drying: Chemical, Morphological and Chemometric Characterization. *Food Chem.* **2018**, *254*, 281−291.

(8) Montero, P.; Calvo, M. M.; Gómez-Guillén, M. C.; Gómez-Estaca, J. Microcapsules Containing Astaxanthin from Shrimp Waste as Potential Food Coloring and Functional Ingredient: Characterization, Stability, and Bioaccessibility. *LWT* **2016**, *70*, 229−236.

(9) de Souza, V. B.; Thomazini, M.; Echalar Barrientos, M. A.; Nalin, C. M.; Ferro-Furtado, R.; Genovese, M. I.; Favaro-Trindade, C. S. Functional Properties and Encapsulation of a Proanthocyanidin-Rich Cinnamon Extract (Cinnamomum Zeylanicum) by Complex Coacervation Using Gelatin and Different Polysaccharides. *Food Hydrocolloids* **2018**, *77*, 297−306.

(10) López-Córdoba, A.; Deladino, L.; Martino, M. Release of Yerba Mate Antioxidants from Corn Starch-Alginate Capsules as Affected by Structure. *Carbohydr. Polym.* **2014**, *99*, 150−157.

(11) Bušić, A.; Belščak-Cvitanović, A.; Vojvodić, A.; Karlović, S.; Kovač, V.; Špoljarić, I.; Mršić, G.; Komes, D. Structuring new alginate network aimed for delivery of dandelion (*Taraxacum officinale* L.) polyphenols using ionic gelation and new filler materials. *Food Res. Int.* **2018**, *111*, 244−255.

(12) Ye, Q.; Li, T.; Li, J.; Liu, L.; Dou, X.; Zhang, X. Development and Evaluation of Tea Polyphenols Loaded Water in Oil Emulsion with Zein as Stabilizer. *J. Drug Delivery Sci. Technol.* **2020**, *56*, 101528.

(13) Gibis, M.; Ruedt, C.; Weiss, J. In Vitro Release of Grape-Seed Polyphenols Encapsulated from Uncoated and Chitosan-Coated Liposomes. *Food Res. Int.* **2016**, *88*, 105−113.

(14) Ramírez-Ambrosi, M.; Caldera, F.; Trotta, F.; Berrueta, L.; Gallo, B. Encapsulation of Apple Polyphenols in β-CD Nanosponges. *J. Inclusion Phenom. Macrocyclic Chem.* **2014**, *80* (1−2), 85−92.

(15) Istenič, K.; Balanč, B. D.; Djordjević, V. B.; Bele, M.; Nedović, V. A.; Bugarski, B. M.; Ulrih, N. P. Encapsulation of Resveratrol into Ca-Alginate Submicron Particles. *J. Food Eng.* **2015**, *167*, 196−203.

(16) Balanč, B.; Kalušević, A.; Drvenica, I.; Coelho, M. T.; Djordjević, V.; Alves, V. D.; Sousa, I.; Moldão-Martins, M.; Rakić, V.; Nedović, V.; et al.et al. Calcium-Alginate-Inulin Microbeads as Carriers for Aqueous Carqueja Extract. *J. Food Sci.* **2016**, *81* (1), No. E65−75.

(17) Belščak-Cvitanović, A.; Komes, D.; Karlović, S.; Djaković, S.; Špoljarić, I.; Mršić, G.; Ježek, D. Improving the Controlled Delivery Formulations of Caffeine in Alginate Hydrogel Beads Combined with Pectin, Carrageenan, Chitosan Psyllium. *Food Chem.* **2015**, *167*, 378−386.

(18) Krishnaiah, Y. S. R.; Karthikeyan, R. S.; Satyanarayana, V. A Three-Layer Guar Gum Matrix Tablet for Oral Controlled Delivery of Highly Soluble Metoprolol Tartrate. *Int. J. Pharm.* **2002**, *241* (2), 353−366.

(19) Talukder, R.; Fassihi, R. Gastroretentive Delivery Systems: Hollow Beads. *Drug Dev. Ind. Pharm.* **2004**, *30* (4), 405−412.

(20) Li, Q.; Duan, M.; Hou, D.; Chen, X.; Shi, J.; Zhou, W. Fabrication and Characterization of Ca (II) -Alginate-Based Beads Combined with Different Polysaccharides as Vehicles for Delivery, Release and Storage of Tea Polyphenols. *Food Hydrocolloids* **2021**, *112*, 106274.

(21) Barnwal, P.; Singh, K. K.; Sharma, A.; Choudhary, A. K.; Saxena, S. N. Influence of Pin and Hammer Mill on Grinding Characteristics, Thermal and Antioxidant Properties of Coriander Powder. *J. Food Sci. Technol.* **2015**, *52* (12), 7783−7794.

(22) Otálora, M. C.; Carriazo, J. G.; Iturriaga, L.; Osorio, C.; Nazareno, M. A. Encapsulating Betalains from *Opuntia ficus-indica* Fruits by Ionic Gelation: Pigment Chemical Stability during Storage of Beads. *Food Chem.* **2016**, *202*, 373−382.

(23) Jinapong, N.; Suphantharika, M.; Jamnong, P. Production of Instant Soymilk Powders by Ultrafiltration, Spray Drying and Fluidized Bed Agglomeration. *J. Food Eng.* **2008**, *84* (2), 194−205.

(24) Parvez, S.; Wani, I. A.; Masoodi, F. A. Extraction Optimization of Green Tea Beverage (Noon Chai) for Yield, Polyphenols and Caffeine Using Response Surface Methodology. *Arab. J. Sci. Eng.* **2022**, *47*, 227−239.

(25) Parvez, S.; Ahmed Wani, I.; Masoodi, F. A. Nanoencapsulation of Green Tea Extract Using Maltodextrin and Its Characterisation. *Food Chem.* **2022**, *384*, 132579.

(26) Rayment, P.; Wright, P.; Hoad, C.; Ciampi, E.; Haydock, D.; Gowland, P.; Butler, M. F. Food Hydrocolloids Investigation of Alginate Beads for Gastro-Intestinal Functionality, Part 1: In Vitro Characterisation. *Food Hydrocolloids* **2009**, *23* (3), 816−822.

(27) Ćujić, N.; Trifković, K.; Bugarski, B.; Ibrić, S.; Pljevljakušić, D.; Šavikin, K. Chokeberry (*Aronia melanocarpa* L.) Extract Loaded in Alginate and Alginate/Inulin System. *Ind. Crops Prod.* **2016**, *86*, 120−131.

(28) Aizpurua-Olaizola, O.; Navarro, P.; Vallejo, A.; Olivares, M.; Etxebarria, N. Microencapsulation and Storage Stability of Polyphenols from Vitis Vinifera Grape Wastes. *Food Chem.* **2016**, *190*, 614−621.

(29) Stojanovic, R.; Belscak-Cvitanovic, A.; Manojlovic, V.; Komes, D.; Bugarski, B. Encapsulation of Thyme (*Thymus serpyllum* L.) Aqueous Extract in Calcium Alginate Beads. *J. Sci. Food Agric.* **2012**, *92*, 685−696.

(30) Pongjanyakul, T.; Rongthong, T. Enhanced entrapment efficiency and modulated drug release of alginate beads loaded with drug−clay intercalated complexes as microreservoirs. *Carbohydr. Polym.* **2010**, *81* (2), 409−419.

(31) Pongjanyakul, T.; Puttipipatkhachorn, S. Xanthan−alginate composite gel beads: Molecular interaction and in vitro characterization. *Int. J. Pharm.* **2007**, *331* (1), 61−71.

(32) Abubakr, N.; Lin, S. X.; Chen, X. D. Effects of Drying Methods on the Release Kinetics of Vitamin B12 in Calcium Alginate Beads. *Drying Technol.* **2009**, *27* (11), 1258−1265.

(33) Arenas, E. H.; Trinidad, T. P. Fate of Polyphenols in Pili (*Canarium ovatum* Engl.) Pomace after in Vitro Simulated Digestion. *Asian Pac. J. Trop. Biomed.* **2017**, *7* (1), 53−58.

(34) Flores, F. P.; Kong, F. In Vitro Release Kinetics of Microencapsulated Materials and the Effect of the Food Matrix. *Annu. Rev. Food Sci. Technol.* **2017**, *8*, 237−259.

(35) Bajpai, S. K.; Sharma, S. Investigation of Swelling/Degradation Behaviour of Alginate Beads Crosslinked with Ca2+ and Ba2+ Ions. *React. Funct. Polym.* **2004**, *59* (2), 129−140.

(36) Tavakol, M.; Vasheghani-Farahani, E.; Dolatabadi-Farahani, T.; Hashemi-Najafabadi, S. Sulfasalazine Release from Alginate-N,O-Carboxymethyl Chitosan Gel Beads Coated by Chitosan. *Carbohydr. Polym.* **2009**, *77* (2), 326−330.

https://doi.org/10.1021/acsfoodscitech.3c00696
ACS Food Sci. Technol. XXXX, XXX, XXX−XXX

(37) Scholt, H. Kinetics of Swelling of Polymers and Their Gels First-Order Swelling Kinetics. *J. Pharm. Sci.* **1992**, *81* (5), 467−470.
(38) Aceval Arriola, N. D.; de Medeiros, P. M.; Prudencio, E. S.; Olivera Müller, C. M.; de Mello Castanho Amboni, R. D. Encapsulation of Aqueous Leaf Extract of Stevia Rebaudiana Bertoni with Sodium Alginate and Its Impact on Phenolic Content. *Food Biosci.* **2016**, *13*, 32−40.
(39) Saénz, C.; Tapia, S.; Chávez, J.; Robert, P. Microencapsulation by Spray Drying of Bioactive Compounds from Cactus Pear (*Opuntia ficus-indica*). *Food Chem.* **2009**, *114* (2), 616−622.
(40) Bakowska-Barczak, A. M.; Kolodziejczyk, P. P. Black Currant Polyphenols: Their Storage Stability and Microencapsulation. *Ind. Crops Prod.* **2011**, *34* (2), 1301−1309.
(41) Huang, X.; Brazel, C. S. On the Importance and Mechanisms of Burst Release in Matrix-Controlled Drug Delivery Systems. *J. Controlled Release* **2001**, *73* (2−3), 121−136.
(42) Belščak-Cvitanović, A.; Stojanović, R.; Manojlović, V.; Komes, D.; Cindrić, I. J.; Nedović, V.; Bugarski, B. Encapsulation of Polyphenolic Antioxidants from Medicinal Plant Extracts in Alginate-Chitosan System Enhanced with Ascorbic Acid by Electrostatic Extrusion. *Food Res. Int.* **2011**, *44* (4), 1094−1101.
(43) Reddy, C. K.; Jung, E. S.; Son, S. Y.; Lee, C. H. Inclusion complexation of catechins-rich green tea extract by β-cyclodextrin: Preparation, physicochemical, thermal, and antioxidant properties. *LWT* **2020**, *131*, 109723.

https://doi.org/10.1021/acsfoodscitech.3c00696
ACS Food Sci. Technol. XXXX, XXX, XXX−XXX